Research Square

Preprints are preliminary reports that have not undergone peer review.
They should not be considered conclusive, used to inform clinical practice,
or referenced by the media as validated information.

Comparative Elicitation Effects of Nickel and Zinc Oxide Nanoparticles on Indole Alkaloid Biosynthesis in in vitro Cultures of Isatis constricta

Özgür KARAKAŞ

okarakas@sirnak.edu.tr

Şırnak Üniversitesi: Sirnak Universitesi https://orcid.org/0000-0003-3339-4811

Nevin ARSLAN

Dicle University: Dicle Universitesi

Fethullah TEKİN

GAP International Agricultural research and Training Center

Alevcan KAPLAN

Dicle University: Dicle Universitesi

Research Article

Keywords: Indirubin, Indigo, Isatis constricta, NiONPs, Tryptanthrin, ZnONPs

Posted Date: January 19th, 2026

DOI: https://doi.org/10.21203/rs.3.rs-8550260/v1

License: This work is licensed under a Creative Commons Attribution 4.0 International License.
Read Full License

Version of Record: A version of this preprint was published at Plant Cell, Tissue and Organ Culture (PCTOC) on April 2nd, 2026. See the published version at https://doi.org/10.1007/s11240-026-03436-9.

Abstract

This study examined the concentration and time-dependent effects of nickel oxide (NiONPs) and zinc oxide (ZnONPs) nanoparticles (0, 10, 25, 50, 75, and 100 mg/L) on the accumulation of indole alkaloids such as indirubin, tryptanthrin, and indigo in Isatis constricta leaf explants cultured in vitro. Exposure to 50 mg/L NiONPs significantly increased the production of tryptanthrin and indirubin during the second week, with roughly 1.6- and 2.3-fold increases compared to the first week. Conversely, indigo levels decreased at all NiONP concentrations, with the greatest reduction observed during prolonged exposure. Similarly, ZnONPs caused notable, concentration-dependent changes in alkaloid production. The highest accumulation of tryptanthrin (2.3-fold) and indirubin (3.4-fold) appeared at 50 mg/L ZnONPs in the second week, while indigo content dropped sharply, especially at 10 mg/L, showing a 1.8-fold decrease compared to the control. Multivariate correlation and chemometric analyses indicated strong links between nanoparticle concentration, exposure time, and metabolite profiles. Overall, these results demonstrate that NiONPs and ZnONPs act as effective abiotic elicitors, influencing indole alkaloid biosynthesis in *I. constricta*, with ZnONPs exhibiting a stronger elicitation effect at optimal doses.

Key message

Nickel and zinc oxide nanoparticles differentially elicit indole alkaloid biosynthesis in under conditions.

Introduction

Plants of the genus *Isatis* (Brassicaceae) have long been valued as natural sources of indigo dye and medicinal materials, particularly in China and several European regions before the late 17th century (Hamburger 2002). These plants contain a wide range of biologically active compounds with antiviral, antimicrobial, antitumoral, and anticarcinogenic properties, as well as traditional uses for treating colds, influenza, and other infections (Meng et al. 2017; Chen et al. 2012; Xi et al. 2018). A considerable number of biologically active pure compounds isolated from natural sources are alkaloids, structurally diverse nitrogen-containing heterocyclic molecules exhibiting alkali-like chemical reactivity and pronounced pharmacological properties. Despite extensive research on their pharmacological effects, the biosynthetic pathways underlying alkaloid formation remain largely unresolved (Palazón et al. 2008). *Isatis* species are known to accumulate various secondary metabolites, including phenolics, flavonoids, and alkaloids (Özel 2018). Among these, indole alkaloids such as indirubin, tryptanthrin, and indigo are particularly notable for their anti-inflammatory and antiviral effects (Zhang et al. 2020; Guo et al. 2020).

Secondary metabolites are essential natural products with significant applications in the food, pharmaceutical, and healthcare industries (Hatami et al. 2019). However, their biosynthesis in nature is often limited and strongly influenced by genetic, environmental, and agronomic factors (Neugart et al. 2018; Vidal-Limon et al. 2018). In vitro culture systems offer an effective platform for the controlled and sustainable production of these compounds, enabling manipulation of metabolic pathways under standardized conditions (Tavan et al. 2023). In this context, elicitor-based strategies have gained

increasing attention as efficient tools for stimulating the accumulation of target secondary metabolites, depending on the type, concentration, and exposure duration of elicitors (Naik and Al-Khayri 2016; Lertphadungkit et al. 2020).

Metal-based nanoparticles (NPs) such as nickel oxide (NiONPs), zinc oxide (ZnONPs), and silver oxide (AgONPs) have recently emerged as potent abiotic elicitors that can enhance the biosynthesis of various classes of plant secondary metabolites (Zhang B et al. 2013). Due to their high surface-to-volume ratio and distinctive physicochemical properties, NPs can interact with plant cells at the molecular level, triggering stress-related signaling cascades and metabolic adjustments (Miri et al. 2017). Several studies have demonstrated that exposure to metallic and metal oxide nanoparticles can modulate the production of alkaloids, phenolics, and flavonoids in *in vitro* cultures of *Hypericum perforatum*, *Brassica juncea*, and *Solanum melongena* (Sharafi et al. 2013; Narendhran et al. 2016; Baskar et al. 2018; Kruszka et al. 2022; Geremew et al. 2023).

Despite the increasing number of studies on nanoparticle-induced changes in plant secondary metabolism, there is limited information about their effect on indole alkaloid biosynthesis in Isatis constricta. Therefore, this study aimed to assess how different concentrations and exposure times of ZnONPs and NiONPs influence the accumulation of three pharmaceutically important indole alkaloids—indirubin, tryptanthrin, and indigo—in I. constricta leaf explants cultured *in vitro*.

Materials and Methods

Plant Samples and Culture Conditions

Mature seeds of *Isatis constricta* were collected from Ergani, Diyarbakır, Turkey (942 m above sea level) and taxonomically identified by Dr. Ömer Saya, Dicle University, Faculty of Science, Department of Biology. The seeds were washed thoroughly with tap water for 5 min, surface-sterilized with 70% ethanol for 45 s, and subsequently immersed in 8% sodium hypochlorite (NaOCl) for 12 min, followed by three to five rinses with sterile distilled water. Surface-sterilized seeds were cultured on Murashige and Skoog (MS) basal medium (Murashige and Skoog 1962) supplemented with 30 g/L sucrose and 6 g L^{-1} agar. The pH of the medium was adjusted to 5.7–5.8 prior to autoclaving at 121°C for 20 min. Six surface-sterilized seeds were inoculated per flask and incubated in a growth chamber under a 16 h light/8 h dark photoperiod at 25 ± 2°C. To maintain culture continuity, germinated seedlings were propagated and subcultured on fresh MS medium until nanoparticle treatments were initiated (Figs. 1a-c).

Applications of ZnONPs and NiONPs

ZnONPs and NiONPs were dispersed in distilled water and sonicated three times for 10 min each, followed by filtration through a 0.45 µm membrane (Merck-Millipore). After four subcultures, healthy plantlets were transferred to freshly prepared MS medium containing varying concentrations of ZnONPs and NiONPs (0, 10, 25, 50, 75, and 100 mg/L). Cultures were exposed to nanoparticles for 14 days. Leaf

samples were collected after 7 and 14 days of exposure to determine the concentrations of indirubin, tryptanthrin, and indigo (Figs. 1b and 1c).

Figure 1 Seedlings propagated in MS Medium containing NiONP*s* and ZnONP*s*. A- Control (Untreated) samples; B- Samples treated 50 ppm NiONP*s*; C- Samples treated 50 ppm ZnONPs

Chemicals and Reagents

Reference standards of tryptanthrin (≥ 98%), indirubin (≥ 98%), and indigo (≥ 98%) were purchased from Sigma-Aldrich (St. Louis, MO, USA). Zinc oxide nanoparticles (ZnONPs; <50 nm, > 97%, nanopowder) were obtained from Sigma-Aldrich Chemie GmbH (Steinheim, Germany), while nickel oxide nanoparticles (NiONPs; <50 nm, > 99.8%, nanopowder, trace metals basis) were supplied by Millipore SAS (Molsheim, France). N, N-Dimethylformamide (DMF), acetonitrile (ACN), and methanol (MeOH), each with a purity of ≥ 99.9%, were purchased from Merck (Darmstadt, Germany). Trifluoroacetic acid (TFA; ≥99%) was obtained from Merck (Hohenbrunn, Germany). HPLC-grade acetonitrile and ultrapure water were used for the preparation of the mobile phase.

Calibration Curves of the Reference Compounds

Reference compounds of indirubin, tryptanthrin, and indigo were dissolved in DMF for preparing of stock solution (1 mg mL^{-1}), and solutions at five different concentrations (10, 25, 50, 75, and 100 mg/L) were prepared by diluting this stock solution with DMF. For generating calibration curves, each reference compound was injected in triplicate into high-pressure liquid chromatography (HPLC).

Extraction of Indirubin, Tryptanthrin, and Indigo

The target compounds (indirubin, tryptanthrin, and Indigo) in *I. constricta* were extracted from leaf explants following a slightly modified version of the method described by Liau et al. (2007). Air-dried leaves were finely powdered using a laboratory mill, and the powdered material was accurately weighed. The samples were sonicated in MeOH (10 mL) at 48°C for 10 min using an ultrasonic device (Jeiotech, US-05, Korea), and this procedure was repeated three times (10 mL × 3). The combined extracts were concentrated under reduced pressure using a rotary evaporator (Labtech EV311). The residues were dissolved in 5 mL of DMF and brought to a final volume of 40 mL with MeOH. The solutions were filtered through 0.45 µm membrane filters (Merck-Millipore®) prior to HPLC analysis.

HPLC Analysis of Indirubin, Tryptanthrin, and Indigo

Quantitative analysis of indirubin, tryptanthrin, and indigo was performed using an HPLC system equipped with an autosampler (SIL-20A HT), a solvent delivery pump (LC-20AT), a photodiode array detector (SPD-M20A PDA), and a degasser (DGU-20A5R). Separation was carried out on an Inertsil ODS-

3 column (5 µm, 4.6 × 250 mm; GL Sciences Inc., Japan) maintained at 30°C. The mobile phase consisted of H_2O and ACN (35:65, v/v) containing 0.1% TFA, delivered at a flow rate of 0.5 mL min^{-1}. The injection volume was 20 µL. Detection wavelengths were set at 275 nm for indirubin, 305 nm for tryptanthrin, and 279 nm for indigo. Retention times for indirubin, tryptanthrin, and indigo were 11.4, 15.2, and 16.2 min, respectively, in leaf explants (Figs. 3a–c).

Statistical Analysis

All experiments were conducted in triplicate. Data were subjected to analysis of variance (ANOVA), and mean comparisons were performed using Duncan's multiple range test at $p \leq 0.05$ (SPSS Software, Version 16.0). Results are expressed as mean ± standard deviation (SD). Additional statistical analyses and visualizations, including hierarchical clustering heatmaps, triangular correlation matrices, and correlation network plots, were conducted using Pearson correlation coefficients with OriginPro 2024b (Academic).

Results and Discussion

Influences of NiONPs on Contents of Indirubin, Tryptanthrin, and Indigo

The effects of exposure times (One and two weeks) and different concentrations (10, 25, 50, 75, and 100 mg/L) of nickel oxide nanoparticles (NiONPs) on the biosynthesis of indirubin, tryptanthrin, and indigo in *Isatis constricta* leaf explants are presented in Figs. 2a–c. HPLC chromatograms confirmed the presence of these compounds according to their reference retention times (Figs. 3a–c).

The results demonstrated that NiONPs significantly influenced secondary metabolite accumulation (indirubin, tryptanthrin, and indigo) in a concentration-dependent manner. Indirubin content increased markedly at 50 mg/L NiONPs during the second week (68.22 ± 1.39 µg/g), corresponding to a 2.29-fold increase compared to the control. However, lower (10–25 mg/L) and higher (75–100 mg/L) concentrations caused a reduction in indirubin levels. Similarly, tryptanthrin production was enhanced at 50 mg/L (9.86 ± 0.15 µg/g), about 1.16-fold higher than the control (8.49 ± 0.10 µg/g), while all other concentrations resulted in decreased accumulation (10, 25, 75, and 100 mg/L) in the second week.

In contrast, indigo production declined under all NiONPs treatments, with the most pronounced decrease observed in the second week, at 50 mg/L (1153.44 ± 19.53 µg/g), showing a 4.35-fold reduction, compared to untreated plantlets (265.18 ± 5.22 µg/g).

Similar trends have been reported in *Brassica rapa* and *Catharanthus vinca*, where NiONPs increased glucosinolate and alkaloid biosynthesis at specific concentration ranges (Chung et al., 2019; Al-Karkhi and Al-Oubaidi 2023). Some studies have reported that the stimulatory effect of NiONPs is not only on alkaloids but also on other compounds in plants (Goharriz et al. 2013). In *Nigella arvensis*, moderate NiONPs exposure enhanced phenolic and iridoid production while excessive doses suppressed saponin

and kaempferol synthesis (Chahardoli et al. 2020; Modarresi et al. 2020) and induced ROS production in tomato (Faisal et al. 2013).

These results collectively suggest that NiONPs act as abiotic elicitors, stimulating secondary metabolism through oxidative signaling and enhanced enzyme activity, although excessive concentrations may trigger stress-induced inhibition in *Nigella arvensis* L (Chahardoli et al., 2020). The opposing patterns of indirubin and tryptanthrin enhancement and indigo reduction may reflect a metabolic redirection within the indole alkaloid biosynthetic pathway.

Nickel induces oxidative stress, disrupts the uptake of essential metal ions, and inhibits nitrogen metabolism, as well as key enzymatic and mitotic activities (Atta et al. 2024). Nickel exposure may compromise multiple metabolic and biochemical functions, potentially disrupting cellular homeostasis (Gajewska and Sklodowska 2008).

Figure 2 The effects of exposure times and different concentrations of NiONP*s* (10, 25, 50, 75, and 100 mg/L) on the production of indirubin, tryptanthrin, and indigo in the leaf explants a- Indirubin, b- Tryptanthrin c- Indigo

Figure 3 HPLC chromatogram of the leaf extracts treated with 50 mg/L of NiONP*s* a- Indirubin, b- Tryptanthrin c- Indigo

Influences of ZnONPs on the Production of Indirubin, Tryptanthrin, and Indigo

The application of zinc oxide nanoparticles (ZnONPs) significantly influenced the biosynthesis of indirubin, tryptanthrin, and indigo in *I. constricta* leaf explants cultured in vitro. The effects were concentration- and time-dependent (Figs. 4a–c). HPLC chromatograms confirmed the presence of these compounds according to their reference retention times (Figs. 5a–c).

ZnONPs treatments enhanced indirubin accumulation at all tested concentrations compared with the control. The greatest increase was observed at 50 mg/L ZnONPs, which resulted in an indirubin concentration of 57.23 ± 1.10 µg/g in the first week—approximately a 2.15-fold increase compared with untreated plantlets (26.58 ± 0.68 µg/g). After two weeks of exposure, indirubin content continued to rise, reaching its maximum at 50 mg/L (90.47 ± 1.47 µg/g), corresponding to a 3.35-fold increase relative to the control (27.02 ± 1.09 µg/g).

Tryptanthrin biosynthesis was also positively affected by ZnONPs treatments. During the first week, all concentrations promoted higher tryptanthrin levels compared with untreated plantlets, with the maximum accumulation occurring at 50 mg/L (15.02 ± 0.05 µg/g), about 1.64-fold higher than the control (9.16 ± 0.08 µg/g). After two weeks, tryptanthrin production further increased, reaching 24.34 ± 0.09 µg/g at 50 mg/L ZnONPs-approximately a 2.27-fold enhancement relative to the control (10.73 ± 0.07 µg/g). These results indicate that ZnONPs can promote sustained stimulation of tryptanthrin biosynthesis. This could be associated with the role of zinc as a cofactor in several enzymatic systems,

particularly those involved in tryptophan-derived alkaloid pathways. Comparable findings were observed by Karakaş (2020), who reported increased indigo and tryptanthrin levels in *Isatis constricta* leaves exposed to silver nanoparticles.

The pronounced increase in metabolite levels implies that ZnO nanoparticles function as abiotic elicitors, potentially activating indole alkaloid biosynthesis via oxidative stress-mediated signaling cascades or by upregulating pivotal biosynthetic enzymes (Alizadeh et al. 2025). The other study by Ambreen et al. (2024) revealed that ZnO nanoparticles act as potent elicitors, triggering thymoquinone biosynthesis in *Nigella sativa* cultures through the upregulation of key enzymatic and regulatory nodes within the metabolic network. Similar stimulatory effects of ZnO-based nanoparticles on secondary metabolite production have been reported in *Stevia rebaudiana* (Kumar et al. 2018) and *Hyoscyamus reticulatus* hairy root cultures (Asl et al. 2018). Exposure to ZnO-NPs was found to alter the indole alkaloid biosynthetic pathway, indicating that ZnO-NPs can influence the secondary metabolic processes in plants (Li et al. 2021). Based on these observations, ZnO nanoparticles may exert comparable elicitor effects in the biosynthetic pathways of alkaloids (Chen et al. 2023).

The application of metal oxide nanoparticles creates stress in plants. In this case, excessive production of reactive oxygen species (ROS) occurs. ROS has several effects, such as inhibition and the production of secondary metabolites in plants. Plants enhance the production of secondary metabolites to protect themselves against the harmful effects of ROS (Sen et al. 2025). The previous research showed that ZnONP*s* were effective on ROS production in *Allium cepa* (Kumari et al. 2011) and *Nicotiana tabacum* L. (Balážová et al. 2020).

In contrast to indirubin and tryptanthrin, indigo accumulation decreased at all concentrations of ZnONPs. After the first week, the lowest indigo content was detected in plantlets treated with 10 mg/L ZnONPs (942.56 ± 13.32 µg/g), corresponding to a 1.23-fold reduction compared with the control (1163.76 ± 9.18 µg/g). This inhibitory effect was more pronounced in the second week, where indigo levels further decreased, reaching 647.02 ± 8.51 µg/g at 10 mg/L, approximately 1.82-fold lower than the control (1178.32 ± 11.29 µg/g). Zinc (Zn) plays a fundamental role in the physiological development of plants, and its contribution to crop nutrition stems from its involvement in numerous enzymatic functions, redox reactions, and metabolic pathways (Semida et al. 2021; Shi et al. 2015). Moreover, Zn acts as a cofactor for enzymes associated with nitrogen assimilation and energy metabolism (Zhang et al. 2019). The impact of zinc (Zn) on plant physiology is modulated by species-dependent characteristics and the specific parameters of experimental design (Oloumi et al. 2015). Among the principal regulatory pathways, zinc (Zn) absorption and its subsequent distribution within plant tissues play a crucial role in determining its functional significance (Shnain et al. 2014).

The reduction in indigo biosynthesis may result from Zn-induced oxidative stress or redirection of metabolic flux toward other indole alkaloids such as indirubin and tryptanthrin. Excess zinc may also suppress key enzymes responsible for indigo formation. The inverse relationship between Zn levels and

alkaloid content in some cases highlights the need for precise micronutrient management, as excessive zinc may inadvertently downregulate their biosynthetic pathways.

Figure 4 The effects of exposure times and different concentrations of ZnONP*s* (10, 25, 50, 75, and 100 mg/L) on the production of indirubin, tryptanthrin, and indigo in the leaf explants a- Indirubin, b- Tryptanthrin, c- Indigo

Figure 5 HPLC chromatogram of the leaf extracts treated with 50 mg/L of ZnONP*s*: a- Indirubin, b- Tryptanthrin, c- Indigo

Correlation analysis among treatments

Correlation analysis is a statistical approach used to quantify the degree and direction of association between two or more quantitative variables. It relies on the assumption of a linear relationship among variables and provides a numerical estimate of this relationship through the correlation coefficient. The Pearson product–moment correlation coefficient (*r*), a dimensionless index ranging from − 1 to + 1, is commonly employed to describe the strength and direction of the relationship. Positive *r* values indicate a direct relationship between the variables, whereas negative values denote an inverse association (Gogtay and Thatte 2017; Sedgwick 2012).

In the present study, a combination of multivariate statistical tools—including hierarchical cluster analysis (HCA) heat maps, triangular Pearson correlation matrices, correlation network plots, and principal component analysis (PCA)-was employed to explore and visualize the relationships among key indole alkaloids (indigo, indirubin, and tryptanthrin) produced under different concentrations and exposure times of ZnONP and NiONP treatments (Figs. 6–9).

The HCA heat map (Fig. 6) revealed distinct clustering patterns among treatments. Two primary clusters were identified: the first encompassed both the first- and second-week treatments of NiONPs and ZnONPs associated with indigo biosynthesis, as well as the first week of ZnONPs for tryptanthrin production. The second cluster included the first and second weeks of ZnONP treatments for indirubin and tryptanthrin production, along with the second week of NiONPs for both tryptanthrin and indirubin synthesis. The first week of NiONPs application for indirubin was positioned as an external branch, indicating a weaker association with the main group.

Treatment concentrations were further separated into three major groups: (i) 75 and 100 mg/L, (ii) 10, 25, and 50 mg/L^{-1}, and (iii) the control. Within the second group, 10 and 25 mg/L formed a distinct subcluster. In control samples, a strong correlation was observed between the first- and second-week applications of both NiONPs and ZnONPs for indigo accumulation, whereas lower correlations were detected among the higher concentrations (10–100 mg/L). Notably, the second week of NiONPs treatment at 50 mg/L showed a strong positive correlation between tryptanthrin and indirubin production. This suggests that, under optimal NiONP exposure, the biosynthetic pathways of these two indole alkaloids may be co-activated or share common regulatory mechanisms.

Figure 6 Hierarchical cluster analysis (HCA) heat map plot (1. WT: First week, 2. WT: Second week, Ing: Indigo, Indrb: Indirubin, Trp: Tryptanthrin, brown color: high correlation and blue color: low correlation) of various treatment data sets of *I.constricta*

Figure 7 Triangle heat map with Pearson correlation matrix analysis of various treatment data sets of *I. constricta* (1. WT: First week, 2. WT: Second week, Ing: Indigo, Indrb: Indirubin, Trp: Tryptanthrin, black color: high correlation and yellow color: low correlation)

As illustrated in Fig. 7, the relationships among variables were analyzed using a triangular heat map based on the Pearson correlation matrix. The Pearson correlation coefficient (*r*) was used to quantify the strength and direction of linear associations between variables, with correlation strength visually represented by color gradients in the heat map (ranging from low to high values). In this analysis, *r* values close to + 1 or − 1 indicate a strong positive or negative relationship, respectively, whereas values near zero suggest weak or no linear association.

The correlation analysis revealed a wide spectrum of interactions, ranging from strong positive to strong negative relationships. Strong positive correlations were observed between the first and second weeks of NiONPs treatment for indigo production (r = 0.99) and between the first week of NiONPs and the first week of ZnONPs treatments for indigo (r = 0.88). Similarly, a strong correlation was detected between the first and second weeks of ZnONPs treatments for indigo (r = 0.97). The second week of NiONPs treatment for indigo also correlated strongly with both the first (r = 0.81) and second weeks (r = 0.92) of ZnONPs treatments.

For indirubin, the first week of NiONPs treatment showed a moderate correlation (r = 0.59) with the first week of ZnONPs, whereas other treatment combinations displayed weak or negative relationships. Notably, the second week of ZnONPs treatment for indirubin exhibited a strong correlation with the second week of NiONPs treatment for tryptanthrin (r = 0.91) and with its own second-week replication (r = 0.98). A moderate correlation was also observed between the second week of ZnONPs treatment for indirubin and the first week of ZnONPs treatment for tryptanthrin (r = 0.56).

In the case of tryptanthrin, a moderate correlation was observed between the first and second weeks of NiONPs treatments (r = 0.59), whereas ZnONPs treatments for tryptanthrin showed a strong correlation across both weeks (r = 0.91). Overall, these results highlight significant interconnections among treatments, suggesting synchronized metabolic responses under specific nanoparticle exposures.

The visual representation of these associations in the correlation network plot (Fig. 8) further clarifies the strength of the relationships, where blue nodes represent high correlations and red nodes indicate low or negative correlations. These findings provide valuable insight into the coordinated behavior of indole alkaloid biosynthesis pathways under nanoparticle elicitation and may serve as a foundation for optimizing future elicitor-based metabolic enhancement studies.

Figure 8 Correlation network plot of various treatment data sets of *I. constricta* (1. WT: First week, 2. WT: Second week, Ing: Indigo, Indrb: Indirubin, Trp: Tryptanthrin, Blue color: high correlation and red color: low correlation).

Figure 9 Principal component analysis (PCA) of various treatment data sets of *I.constricta* (1. WT: First week, 2. WT: Second week, Ing: Indigo, Indrb: Indirubin, Trp: Tryptanthrin)

Notably, as shown in the PCA biplot (Fig. 9), the first two principal components (PC1 and PC2) together accounted for 82.2% of the total variance among treatments, indicating that the majority of the data variability was effectively captured by these two components. PC1 explained 56.59% of the variance, while PC2 contributed an additional 25.63%. The clustering pattern observed in the PCA plot was consistent with the correlation analyses, confirming the close associations among related variables.

The control group was distinctly separated from all nanoparticle treatments, reflecting its unique metabolic profile. Treatments with higher nanoparticle concentrations (75 and 100 mg/L) were positioned in the lower-left quadrant of the plot, clustering with the first week of indirubin–NiONPs (IndrbNiONPs) and both the first and second weeks of indirubin–ZnONPs (IndrbZnONPs) treatments. This grouping suggests that higher concentrations of nanoparticles exerted similar influences on indirubin accumulation, contributing substantially to the variance explained by PC1. In contrast, moderate concentrations (10, 25, and 50 mg/L) were located in the upper-left quadrant, forming a distinct cluster that represented a separate response pattern associated with differential metabolite production.

These results indicate that nanoparticle concentration and exposure duration are the primary factors driving variability in the biosynthesis of indole alkaloids, with PCA effectively differentiating treatment-specific metabolic responses in *Isatis constricta* leaf explants.

Conclusion

This study demonstrated that NiONPs and ZnONPs differentially influenced indole alkaloid biosynthesis in *Isatis constricta* leaf explants cultured *in vitro*. Moderate concentrations of both nanoparticles markedly enhanced the production of indirubin and tryptanthrin, whereas higher concentrations inhibited their synthesis and reduced indigo accumulation. This trend suggests a nanoparticle-induced metabolic redirection favoring specific branches of the indole alkaloid pathway.

Multivariate correlation and chemometric analyses supported these results, revealing strong positive associations between nanoparticle concentration and indirubin/tryptanthrin levels, along with a negative relationship with indigo. Overall, NiONPs and ZnONPs appear to act as effective nanoelicitors that can selectively stimulate the accumulation of pharmaceutically valuable alkaloids in *I. constricta* under optimized *in vitro* conditions.

Abbreviations

NiONPs
Nickel oxide nanoparticles
ZnONPs
Zinc oxide nanoparticles
NaOCl
Sodium hypochlorite
MS
Murashige-Skoog
DMF
N, N-dimethyl formamide
ACN
Acetonitrile
MeOH
Methanol
TFA
Trifluoroacetic acid
HPLC
High-pressure liquid chromatography
HCA
Hierarchical cluster analysis
PCA
principal component analysis
1. WT
First week
2. WT
Second week
Indrb
Indirubin
Trp
Tryptanthrin
Ing
Indigo
r
The Pearson correlation coefficient

Declarations

Competing Interests:

The authors have no relevant financial or non-financial interests to disclose.

Contributions of Authors

Özgür Karakaş contributed to drafting the working, carrying out of analysis, and plant tissue culture. Nevin Arslan contributed to the performance of the analysis and plant tissue culture. Alevcan Kaplan contributed to the performance of the analysis. Fethullah Tekin contributed to providing the plant samples.

Ethics declaration

This article does not contain any studies with human participants or animals performed by any of the authors.

Funding:

This work was supported by Sirnak University Research Project Council (Grant Number: 2017.04.08.01).

Acknowledgements

This work was supported by the Şırnak University Research Project Council (Grant No. 2017.04.08.01).

Availability of Data and Materials:

All data generated or analyzed during this study are included in this published article and its supplementary information files.

References

1. Al-Karkhi MAA, Al-Oubaidi HKM (2023) Effect of NiO nanoparticles on increasing medical compounds (alkaloids) of *Catharanthus vinca* (L.) G. Don in callus in vitro. Int J Drug Deliv Technol 13(2):675–678. https://doi.org/10.25258/ijddt.13.2.32
2. Alizadeh S, Hosseini B, Hemmati S, Tahmasebi R (2025) The high production of tropane alkaloids in hairy roots of *Hyoscyamus reticulatus* L. elicited by ZnO NPs in a bioreactor condition. Sci Rep 15:17218. https://doi.org/10.1038/s41598-025-17218
3. Ambreen, Khan MA, Raza A, Yousaf R, Ali H, Darwish H (2024) Impact of zinc oxide nanoparticles on biosynthesis of thymoquinone in cell cultures of *Nigella sativa*. Plant Nano Biol 10:100109. https://doi.org/10.1016/j.plana.2024.100109
4. Asl KR, Hosseini B, Sharafı A, Palazon J (2018) Influence of nano-zinc oxide on tropane alkaloid production, h6h gene transcription and antioxidant enzyme activity in *Hyoscyamus reticulatus* L. hairy roots. Eng Life Sci 19(1):73–89. https://doi.org/10.1002/elsc.201800087

5. Atta N, Shahbaz M, Farhat F, Maqsood MF, Zulfiqar U, Naz N, Ahmed MM, Hassan NU, Mujahid N, Mustafa AEMA, Elshikh MS, Chaudhary T (2024) Proline-mediated redox regulation in wheat for mitigating nickel-induced stress and soil decontamination. *Sci Rep* 14, 456 (2024). https://doi.org/10.1038/s41598-023-50576-5
6. Balážová Ľ, Baláž M, Babula P (2020) Zinc oxide nanoparticles damage tobacco BY-2 cells by oxidative stress followed by processes of autophagy and programmed cell death. Nanomaterials 10(6):1066. https://doi.org/10.3390/nano10061066
7. Baskar V, Nayeem S, Kuppuraj SP, Muthu T, Ramalingam S (2018) Assessment of the effects of metal oxide nanoparticles on the growth, physiology and metabolic responses in in vitro grown eggplant (*Solanum melongena*). 3 Biotech 8(8):362. https://doi.org/10.1007/s13205-018-1386-9
8. Chahardoli A, Karimi N, Ma X, Qalekhani F (2020) Effects of engineered aluminum and nickel oxide nanoparticles on the growth and antioxidant defense systems of *Nigella arvensis* L. Sci Rep 10:3847. https://doi.org/10.1038/s41598-020-60841-6
9. Chen C, Zhao Y, Wang D, Ren Y, Liu H, Tian Y, Geng Y, Tang Y, Chen X (2023) Effects of nanoscale zinc oxide treatment on growth, rhizosphere microbiota, and metabolism of *Aconitum carmichaelii*. PeerJ 11:e16177. https://doi.org/10.7717/peerj.16177
10. Chen MH, Lin S, Li L, Zhu CG, Wang X, Wang Y, Jiang B, Wang S, Li Y, Jiang J, Shi J (2012) Enantiomers of an indole alkaloid containing unusual dihydrothiopyran and 1,2,4-thiadiazole rings from the root of *Isatis indigotica*. Org Lett 14(22):5668–5671. https://doi.org/10.1021/ol302660t
11. Chung IM, Venkidasamy B, Thiruvengadam M (2019) Nickel oxide nanoparticles cause substantial physiological, phytochemical, and molecular-level changes in Chinese cabbage seedlings. Plant Physiol Biochem 139:92–101. https://doi.org/10.1016/j.plaphy.2019.03.010
12. Faisal M, Saquib Q, Alatar AA, Al-Khedhairy AA, Hegazy AK, Musarrat J (2013) Phytotoxic hazards of NiO nanoparticles in tomato: a study on mechanism of cell death. J Hazard Mater 250–251:318–332. https://doi.org/10.1016/j.jhazmat.2013.01.063
13. Gajewska E, Skłodowska M (2008) Differential biochemical responses of wheat shoots and roots to nickel stress: antioxidative reactions and proline accumulation. Plant Growth Regul 54:179–188. https://doi.org/10.1007/s10725-007-9240-9
14. Geremew A, Carson L, Woldesenbet S, Wang H, Reeves S, Brooks N Jr, Saganti P, Weerasooriya A, Peace E (2023) Effect of zinc oxide nanoparticles synthesized from Carya illinoinensis leaf extract on growth and antioxidant properties of mustard (*Brassica juncea*). Front Plant Sci 14:1108186. https://doi.org/10.3389/fpls.2023.1108186
15. Gogtay NJ, Thatte UM (2017) Principles of correlation analysis. J Assoc Physicians India 65(3):78–81
16. Goharriz LY, Rajaei P, Moradalizdeh M (2015) Effect of different concentrations of nickel on some secondary metabolites in coriander (*Coriandrum sativum* L). Int J Life Sci 9(2):28–32. https://doi.org/10.3126/ijls.v9i2.12059

17. Guo Q, Li D, Xu C, Zhu C, Guo Y, Yu H, Wang X, Shi J (2020) Indole alkaloid glycosides with a 1'-(phenyl)ethyl unit from *Isatis indigotica* leaves. Acta Pharm Sin B 10(5):895–902. https://doi.org/10.1016/j.apsb.2019.09.001
18. Hamburger M (2002) *Isatis tinctoria*-from the rediscovery of an ancient medicinal plant towards a novel anti-inflammatory phytopharmaceutical. Phytochem Rev 1(3):333–344. https://doi.org/10.1023/A:1026095608691
19. Hatami M, Badi HN, Ghorbanpour M (2019) Nano-elicitation of secondary pharmaceutical metabolites in plant cells: a review. J Med Plants 18(71):6–37. https://doi.org/10.29252/JMP.3.71.6
20. Karakaş Ö (2020) Effect of silver nanoparticles on production of indole alkaloids in *Isatis constricta*. Iran J Sci Technol Trans Sci 44:621–627. https://doi.org/10.1007/s40995-020-00878-4
21. Kruszka D, Selvakesavan RK, Kachlicki P, Franklin G (2022) Untargeted metabolomics analysis reveals the elicitation of important secondary metabolites upon treatment with various metal and metal oxide nanoparticles in *Hypericum perforatum* L. cell suspension cultures. Ind Crops Prod 178:114561. https://doi.org/10.1016/j.indcrop.2022.114561
22. Kumar V, Sachdev D, Pasricha R, Maheshwari PH, Taneja NK (2018) Zinc-supported multiwalled carbon nanotube nanocomposite: a synergism to micronutrient release and a smart distributor to promote growth of onion seeds in arid conditions. ACS Appl Mater Interfaces 10(43):36733–36745. https://doi.org/10.1021/acsami.8b13464
23. Kumari M, Khan SS, Pakrashi S, Mukherjee A, Chandrasekaran N (2011) Cytogenetic and genotoxic effects of zinc oxide nanoparticles on root cells of *Allium cepa*. J Hazard Mater 190(1–3):613–621. https://doi.org/10.1016/j.jhazmat.2011.03.095
24. Lertphadungkit P, Suksiriworapong J, Satitpatipan V, Sirikantaramas S, Wongrakpanich A, Bunsupa S (2020) Enhanced production of bryonolic acid in *Trichosanthes cucumerina* L. (Thai cultivar) cell cultures by elicitors and their biological activities. Plants 9(6):709. https://doi.org/10.3390/plants9060709
25. Li S, Liu J, Wang Y, Gao Y, Zhang Z, Xu J, Xing G (2021) Comparative physiological and metabolomic analyses revealed that foliar spraying with zinc oxide and silicon nanoparticles modulates metabolite profiles in cucumber (*Cucumis sativus* L). Food Energy Secur 10(4):e269. https://doi.org/10.1002/fes3.269
26. Liau BC, Jong TT, Lee MR, Chen SS (2007) LC-APCI-MS method for detection and analysis of tryptanthrin, indigo, and indirubin in daqingye and banlangen. J Pharm Bıomed Anal 43(1):346–351. https://doi.org/10.1016/j.jpba.2007.02.030
27. Meng LJ, Guo QL, Liu YF, Shi JG (2017) 8,4'-Oxyneolignane glucosides from an aqueous extract of ban lan gen (*Isatis indigotica* root) and their absolute configurations. Acta Pharm Sin B 7(6):638–646. https://doi.org/10.1016/j.apsb.2017.09.006
28. Miri A, Shakib E, Ebrahimi O, Sharifi-Rad J (2017) Impacts of nickel nanoparticles on growth characteristics, photosynthetic pigment content and antioxidant activity of *Coriandrum sativum* L. Orient J Chem 33(3):1297–1303. http://dx.doi.org/10.13005/ojc/330329

29. Modarresi M, Chahardoli A, Karimi N, Chahardoli S (2020) Variations of glaucine, quercetin and kaempferol contents in *Nigella arvensis* against Al_2O_3, NiO, and TiO_2 nanoparticles. Heliyon 6(6):e04265. https://doi.org/10.1016/j.heliyon.2020.e04265
30. Murashige T, Skoog F (1962) A revised medium for rapid growth and bioassays with tobacco tissue cultures. Physiol Plant 15(3):473–497. https://doi.org/10.1111/j.1399-3054.1962.tb08052.x
31. Naik PM, Al-Khayri JM (2016) Abiotic and biotic elicitors-role in secondary metabolites production through in vitro culture of medicinal plants. In: Shanker AK, Shanker C (eds) Abiotic and Biotic Stress in Plants: Recent Advances and Future Perspectives. InTechOpen, London. https://doi.org/10.5772/61442
32. Narendhran S, Rajiv P, Sivaraj R (2016) Influence of zinc oxide nanoparticles on growth of *Sesamum indicum* L. in zinc deficient soil. Int J Pharm Pharm Sci 8:365–371
33. Neugart S, Baldermann S, Hanschen FS et al (2018) The intrinsic quality of brassicaceous vegetables: how secondary plant metabolites are affected by genetic, environmental, and agronomic factors. Sci Hortic 233:460–478. https://doi.org/10.1016/j.scienta.2017.12.038
34. Oloumi H, Soltaninejad R, Baghizadeh A (2015) The comparative effects of nano and bulk size particles of CuO and ZnO on glycyrrhizin and phenolic compounds in *Glycyrrhiza glabra* L. seedlings. Indian J Plant Physiol 20:157–161. https://doi.org/10.1007/s40502-015-0143-x
35. Özel ÇA (2018) Efficient in vitro plant regeneration from cultured leaf and petiole explants of *Isatis constricta* Davis. Acta Sci Pol Hortorum Cultus 17(3):49–55. https://doi.org/10.24326/asphc.2018.3.5
36. Palazón J, Navarro-Ocaña A, Hernández-Vázquez L, Mirjalili MH (2008) Application of metabolic engineering to the production of scopolamine. Molecules 13(8):1722–1742. https://doi.org/10.3390/molecules13081722
37. Sedgwick P (2012) Pearson's correlation coefficient. BMJ 345:e4483. https://doi.org/10.1136/bmj.e4483
38. Semida WM, Abdelkhalik A, Mohamed G, El-Mageed A, Taia A, El-Mageed A, Shimaa A, Rady MM, Ali EF (2021) Foliar application of zinc oxide nanoparticles promotes drought stress tolerance in eggplant (*Solanum melongena* L). Plants 10(2):421. https://doi.org/10.3390/plants10020421
39. Sen B, Roy D, Narayan M, Sarma H (2025) Nanoparticle-driven stress alleviation: exploring the roles of metal and metal oxide nanoparticles in plant abiotic stress management. Discov Plants 2:74. https://doi.org/10.1007/s44372-025-00153-z
40. Sharafı E, Khayam Nekoei SM, Fotokian MH, Davoodi D, Mirzaei HH, Hasanloo T (2013) Improvement of hypericin and hyperforin production using zinc and iron nano-oxides as elicitors in cell suspension culture of St. John's wort (*Hypericum perforatum* L). J Med Plants By-Prod 2:177–184
41. Shi WG, Li H, Liu TX, Polle A, Peng CH, Luo ZB (2015) Exogenous abscisic acid alleviates zinc uptake and accumulation in *Populus canescens* exposed to excess zinc. Plant Cell Environ 38(1):207–223. https://doi.org/10.1111/pce.12434

42. Shnain R, Prasad V, Saravanan S (2014) Effect of zinc and boron on growth, yield and quality of tomato (*Lycopersicon esculentum* Mill.) cv. Heem Sohna under protected cultivation. Eur Acad Res 2(3):78–79
43. Tavan M, Hanachi P, Mirjalili MH (2023) Biochemical changes and enhanced accumulation of phenolic compounds in cell culture of Perilla frutescens (L.) by nano-chemical elicitation. Plant Physiol Biochem 204:108151. https://doi.org/10.1016/j.plaphy.2023.108151
44. Vidal-Limon H, Sanchez-Muñoz R, Khojasteh A, Moyano E, Cusido RM, Palazón J (2017) Taxus cell cultures: an effective biotechnological tool to enhance and gain new biosynthetic insights into taxane production. In: Pavlov A, Bley T (eds) Bioprocessing of Plant In Vitro Systems. Springer, Cham. https://doi.org/10.1007/978-3-319-54600-1_5
45. Xi YF, Zhou L, Bai M, Wang J, Lin B et al (2018) N-acylanthranilic acid derivatives with anti-Aβ1–42 aggregation activity from the leaves of *Isatis indigotica* fortune. Fitoterapia 128:169–174. https://doi.org/10.1016/j.fitote.2018.05.025
46. Zhang B, Zheng LP, Li Y, Wang J (2013) Stimulation of artemisinin production in *Artemisia annua* hairy roots by Ag–SiO_2 core–shell nanoparticles. Curr Nanosci 9(3):363–370. https://doi.org/10.2174/1573413711309030012
47. Zhang D, Sun Y, Chen Z, Jia Q, Zhu W, Chen K, Li Y, Wang R (2020) Bisindole alkaloids with nitric oxide inhibitory activities from an alcohol extract of the *Isatis indigotica* roots. Fitoterapia 146:104654. https://doi.org/10.1016/j.fitote.2020.104654
48. Zhang J, Wang S, Song S, Xu F, Pan Y, Wang H (2019) Transcriptomic and proteomic analyses reveal new insight into chlorophyll synthesis and chloroplast structure of maize leaves under zinc deficiency stress. J Proteom 199:123–134. https://doi.org/10.1016/j.jprot.2019.03.001

Figures

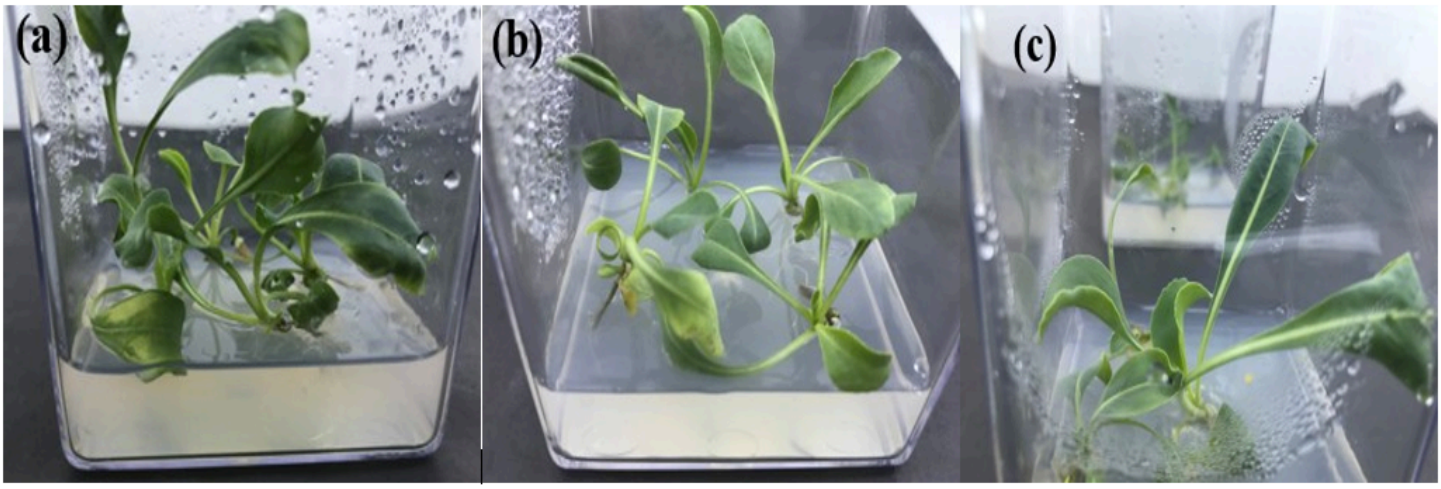
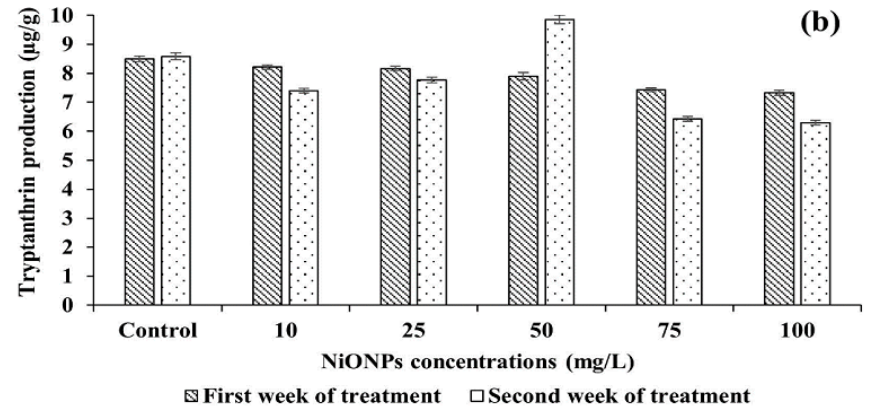
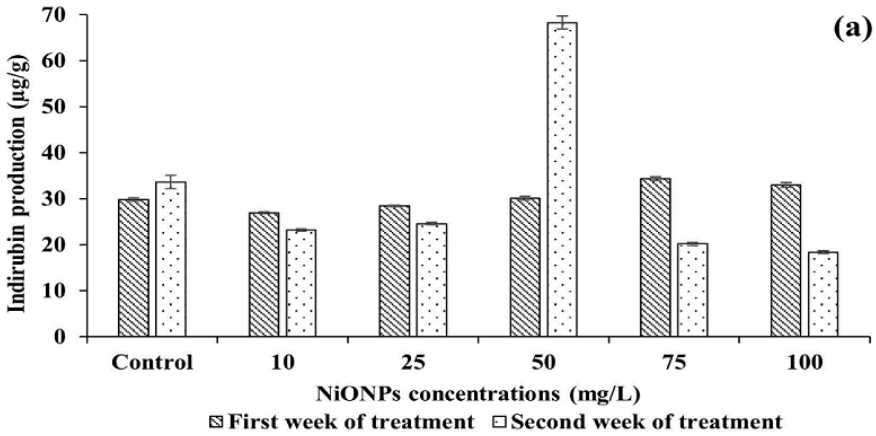


Figure 1

Seedlings propagated in MS Medium containing NiONP*s*and ZnONP*s*. A- Control (Untreated) samples; B- Samples treated 50 ppm NiONP*s*; C- Samples treated 50 ppm ZnONPs





ZnONPs

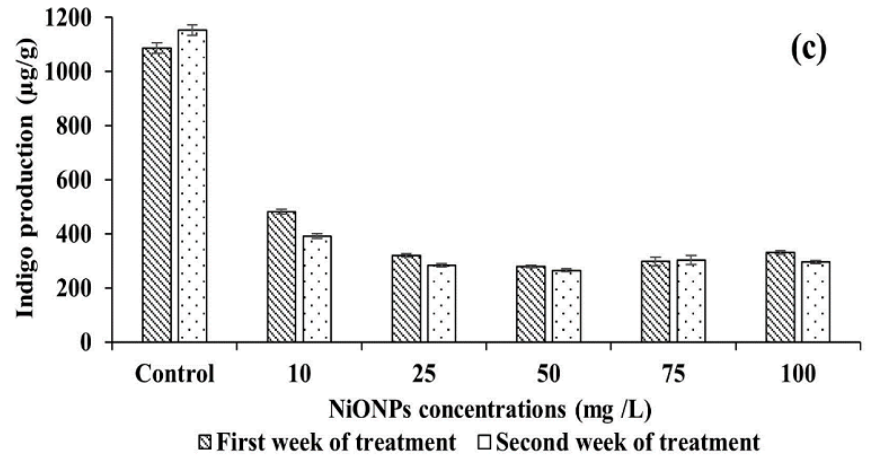


Figure 2

The effects of exposure times and different concentrations of NiONP*s* (10, 25, 50, 75, and 100 mg/L) on the production of indirubin, tryptanthrin, and indigo in the leaf explants a- Indirubin, b- Tryptanthrin c- Indigo

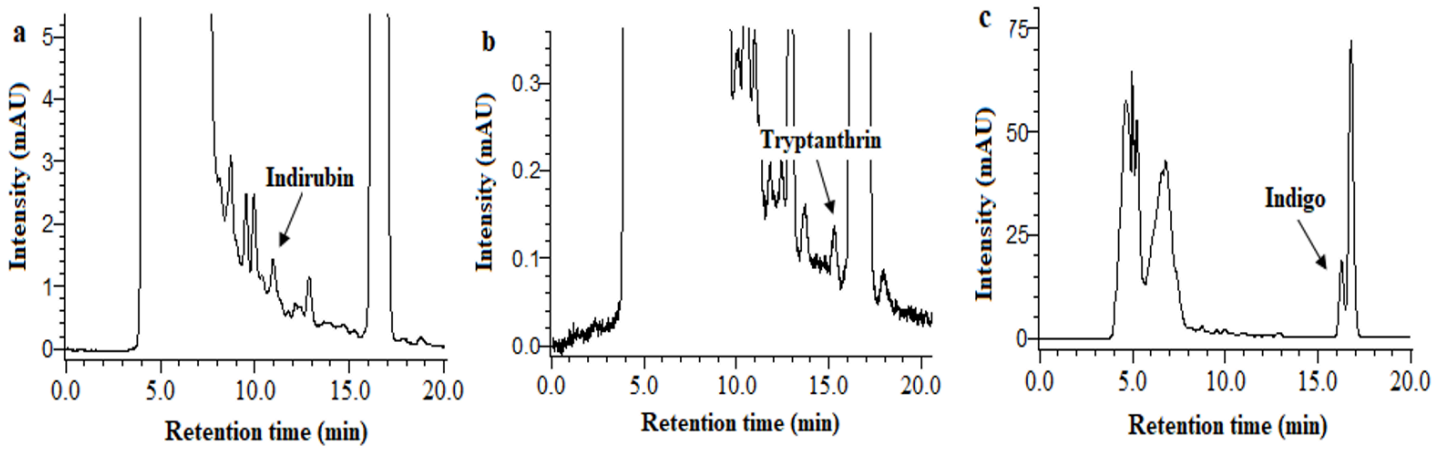


Figure 3

HPLC chromatogram of the leaf extracts treated with 50 mg/L of NiONP*s* a- Indirubin, b- Tryptanthrin c- Indigo

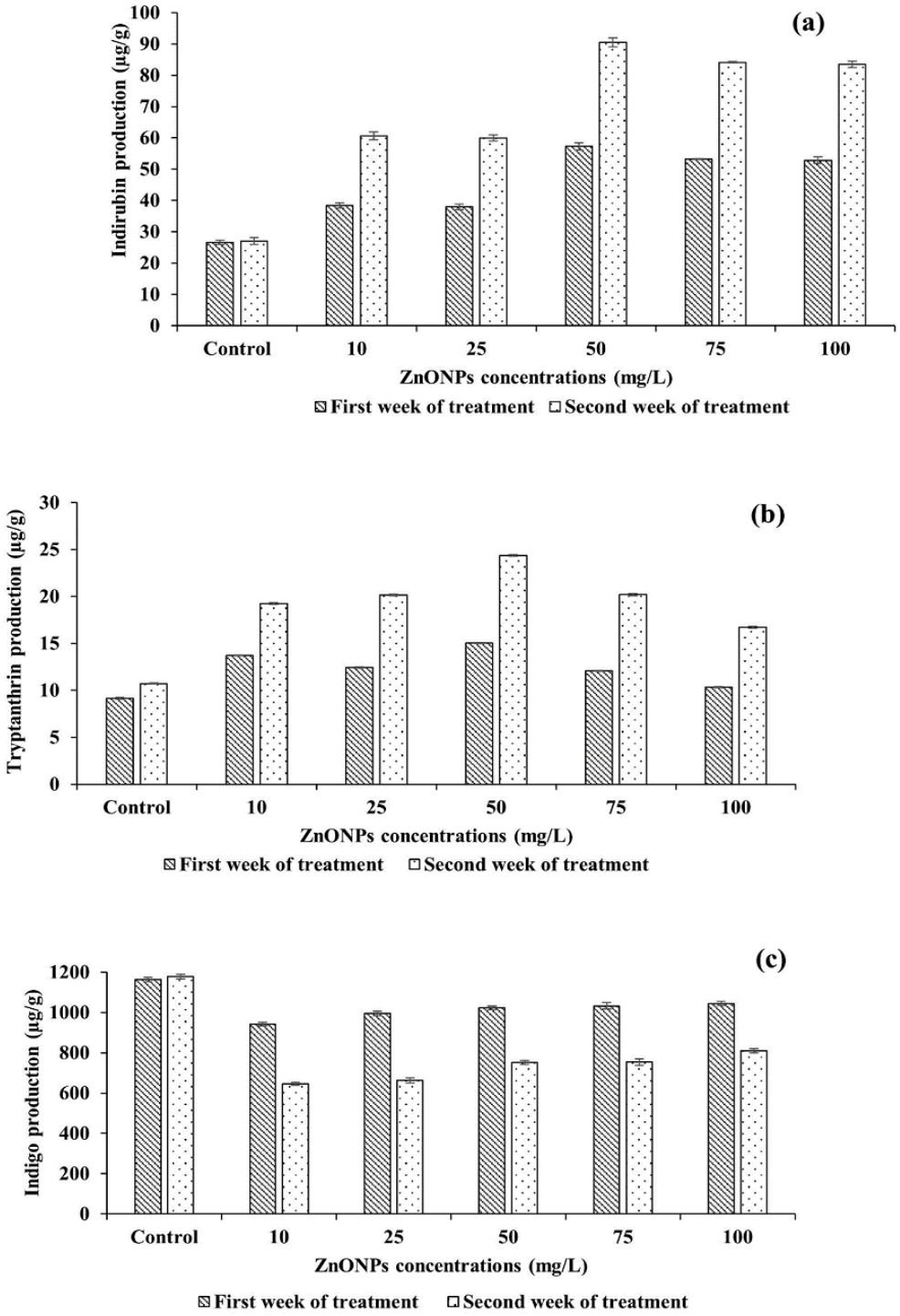


Figure 4

The effects of exposure times and different concentrations of ZnONP*s*(10, 25, 50, 75, and 100 mg/L) on the production of indirubin, tryptanthrin, and indigo in the leaf explants a- Indirubin, b- Tryptanthrin, c- Indigo

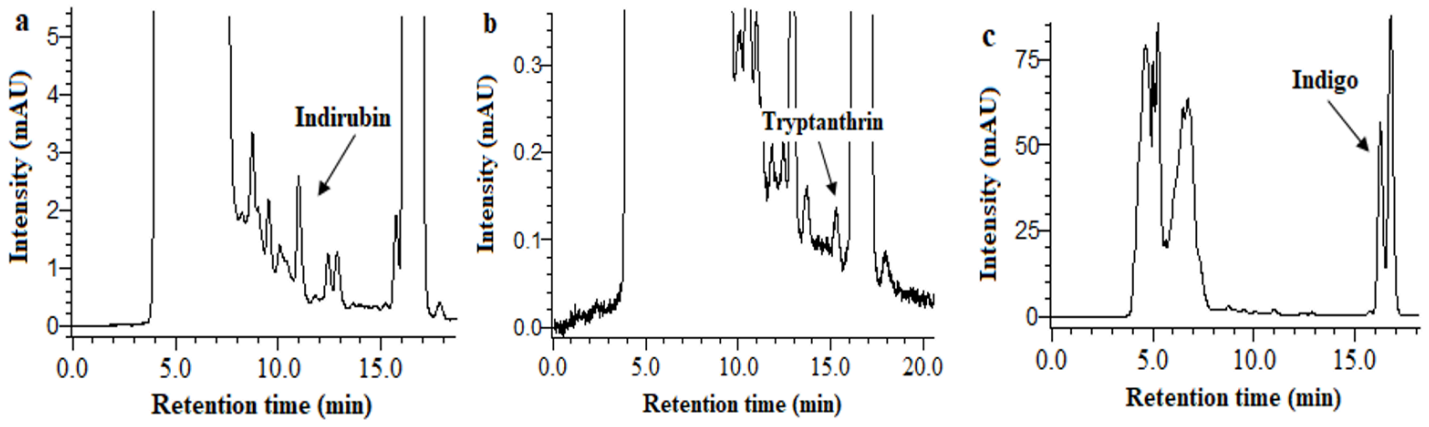


Figure 5

HPLC chromatogram of the leaf extracts treated with 50 mg/L of ZnONP*s*:a- Indirubin, b- Tryptanthrin, c- Indigo

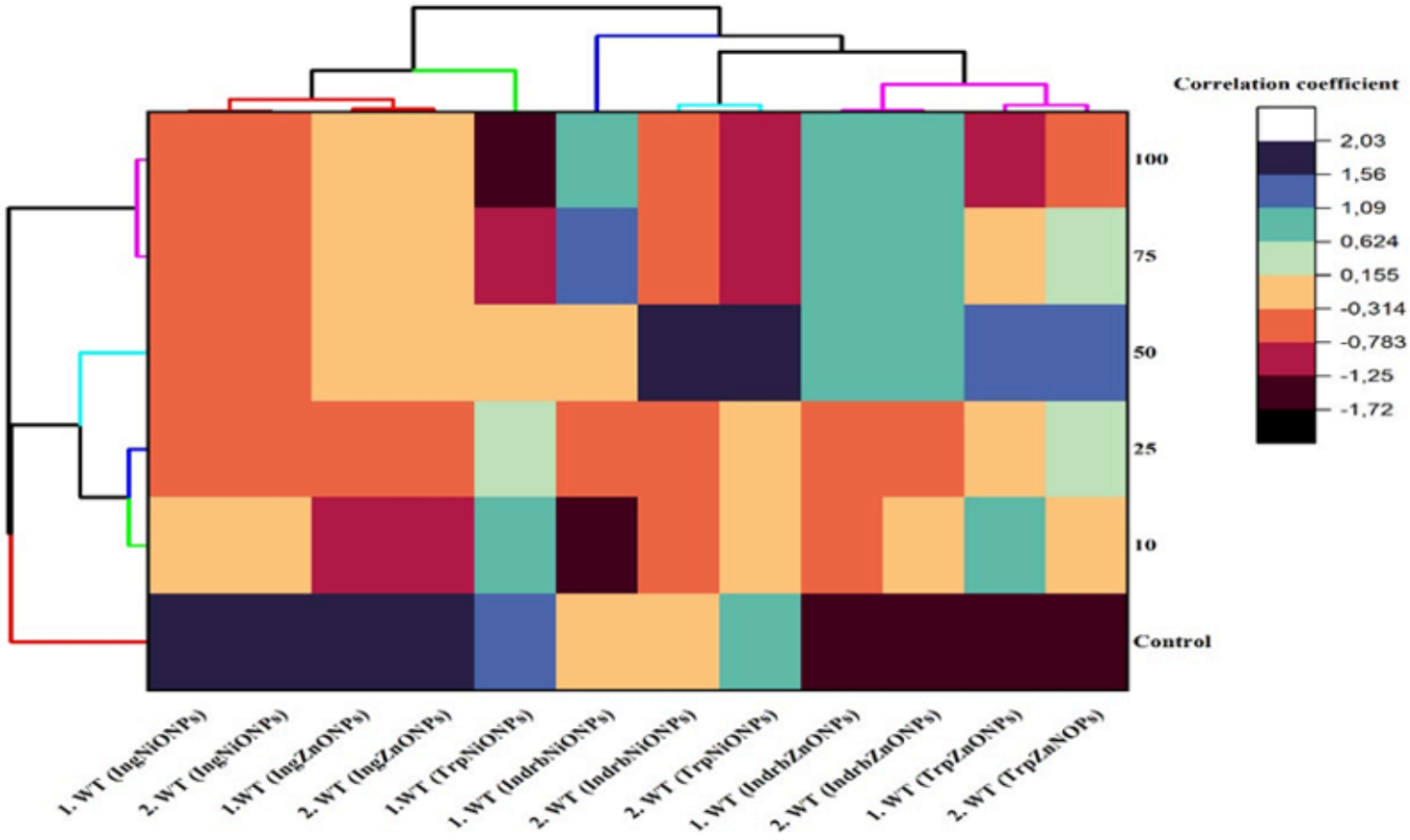


Figure 6

Hierarchical cluster analysis (HCA) heat map plot (1. WT: First week, 2. WT: Second week, Ing: Indigo, Indrb: Indirubin, Trp: Tryptanthrin, brown color: high correlation and blue color: low correlation) of various treatment data sets of *I.constricta*

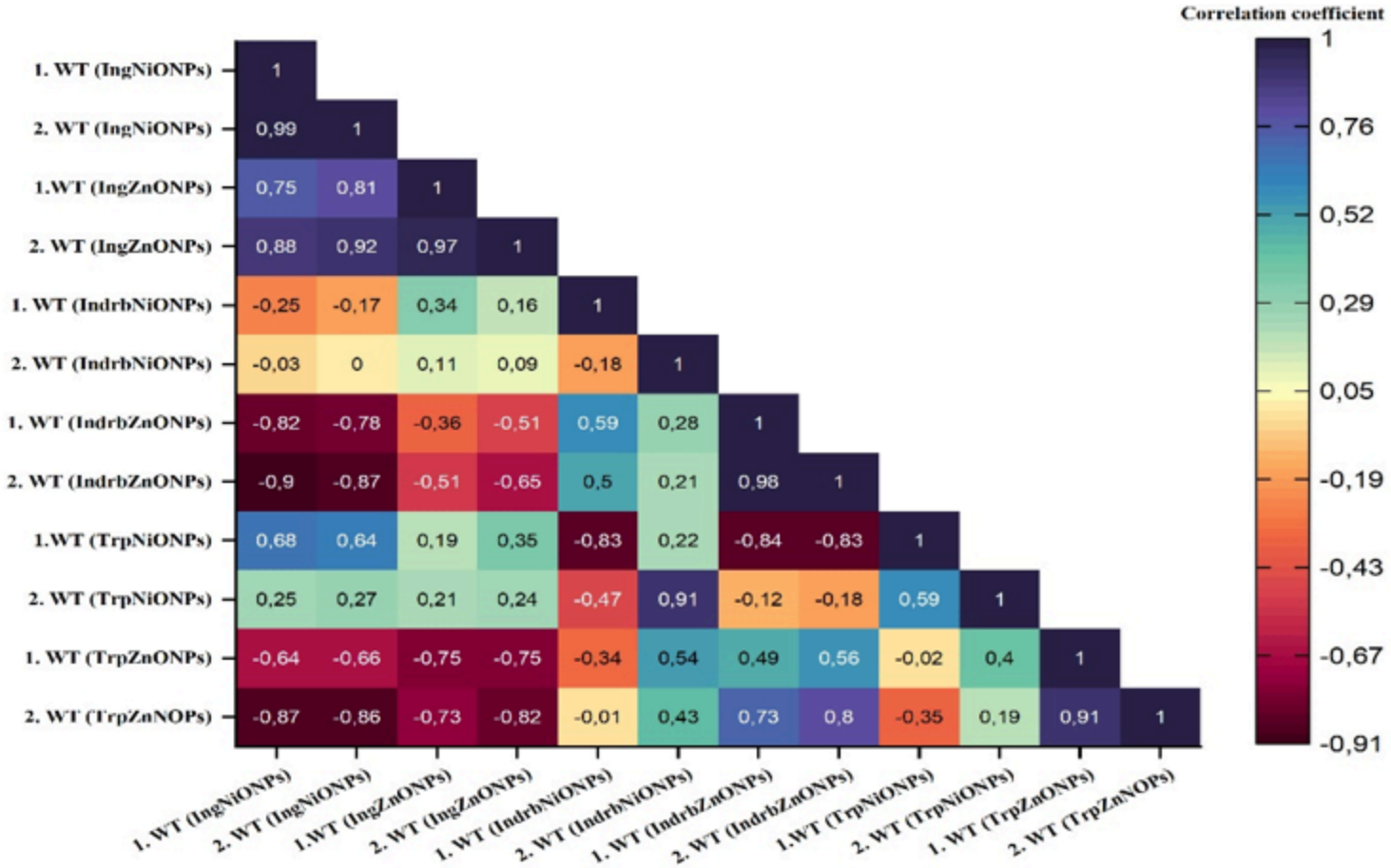


Figure 7

Triangle heat map with Pearson correlation matrix analysis of various treatment data sets of *I. constricta* (1. WT: First week, 2. WT: Second week, Ing: Indigo, Indrb: Indirubin, Trp: Tryptanthrin, black color: high correlation and yellow color: low correlation)

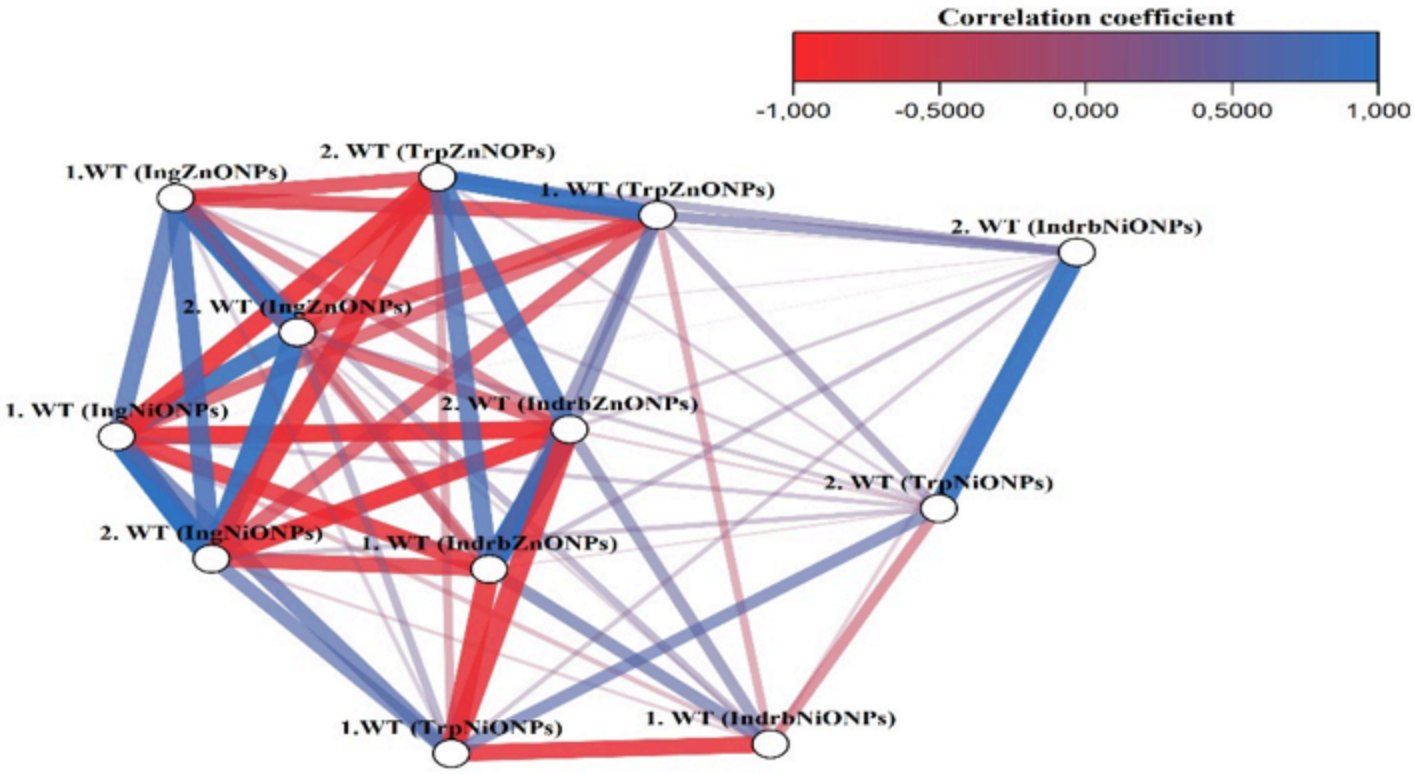


Figure 8

Correlation network plot of various treatment data sets of *I. constricta* (1. WT: First week, 2. WT: Second week, Ing: Indigo, Indrb: Indirubin, Trp: Tryptanthrin, Blue color: high correlation and red color: low correlation).

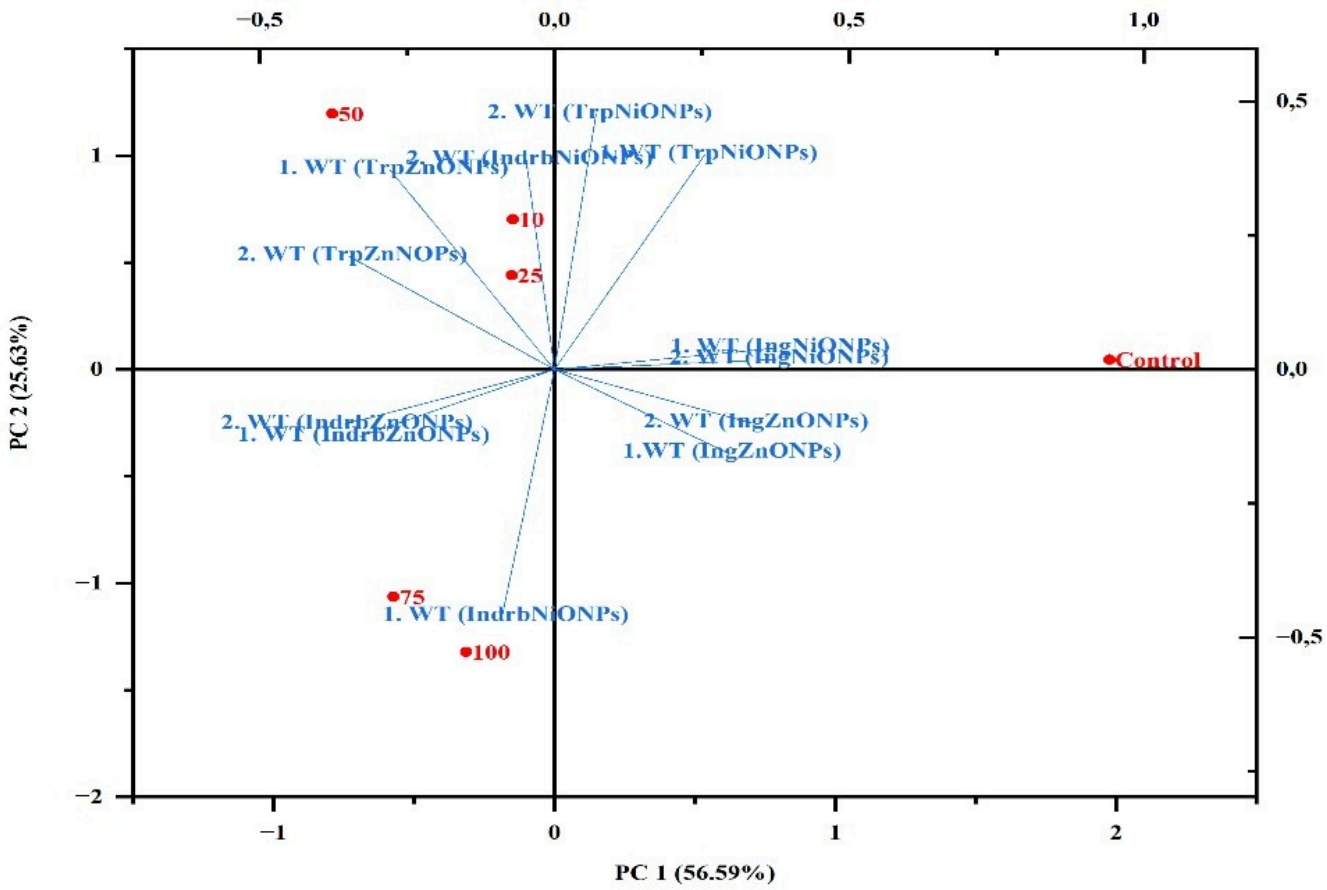


Figure 9

Principal component analysis (PCA) of various treatment data sets of *I.constricta* (1. WT: First week, 2. WT: Second week, Ing: Indigo, Indrb: Indirubin, Trp: Tryptanthrin)

Supplementary Files

This is a list of supplementary files associated with this preprint. Click to download.

- Graphicalabstractandtitlepage.docx